arXiv:2410.13848v1 [cs.CV] 17 Oct 2024

Janus: Decoupling Visual Encoding for Unified Multimodal Understanding and Generation

Chengyue Wu[1,2] Xiaokang Chen[1,*,†] Zhiyu Wu[1,3] Yiyang Ma[1,3] Xingchao Liu[1] Zizheng Pan[1]
Wen Liu[1] Zhenda Xie[1] Xingkai Yu[1] Chong Ruan[1] Ping Luo[2,*]

[1]**DeepSeek-AI** [2]**The University of Hong Kong** [3]**Peking University**
[†]**: Project lead** [*]**: Corresponding authors**
Project Page: https://github.com/deepseek-ai/Janus

Abstract

In this paper, we introduce **Janus**, an autoregressive framework that unifies multimodal understanding and generation. Prior research often relies on a single visual encoder for both tasks, such as Chameleon. However, due to the differing levels of information granularity required by multimodal understanding and generation, this approach can lead to suboptimal performance, particularly in multimodal understanding. To address this issue, we decouple visual encoding into separate pathways, while still leveraging a single, unified transformer architecture for processing. The decoupling not only alleviates the conflict between the visual encoder's roles in understanding and generation, but also enhances the framework's flexibility. For instance, both the multimodal understanding and generation components can independently select their most suitable encoding methods. Experiments show that Janus surpasses previous unified model and matches or exceeds the performance of task-specific models. The simplicity, high flexibility, and effectiveness of Janus make it a strong candidate for next-generation unified multimodal models.

1. Introduction

In recent years, multimodal large models have made significant advancements in both understanding and generation domains [20, 51]. In the field of multimodal understanding, researchers follow the design of LLaVA [51] by using a vision encoder as a bridge to enable large language models (LLMs) to understand images. In the field of visual generation, diffusion-based approaches [9, 20, 20, 67] have seen notable success. More recently, some works have explored autoregressive methods for vision generation [73, 79], achieving performance comparable to diffusion models. To build more powerful and generalist multimodal models, researchers have sought to combine multimodal understanding and generation tasks [75, 77, 94]. For instance, some studies have attempted to connect multimodal understanding models with pretrained diffusion models [27, 28, 75]. For example, Emu [75] uses the output of the LLM as a condition for a pretrained diffusion model, and then relies on the diffusion model to generate images. However, strictly speaking, this approach cannot be considered a truly unified model, because the visual generation functionality is handled by the external diffusion model, while the multimodal LLM itself lacks the capability to directly generate images.

Other approaches [77, 85, 86, 94] employ a single transformer to unify both multimodal un-

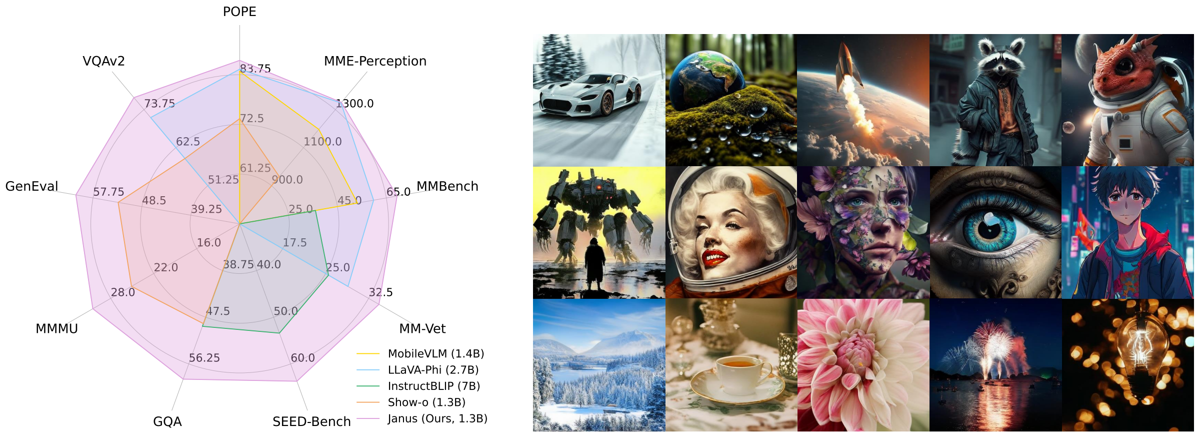

(a) Benchmark Performance.

(b) Visual Generation Results.

Figure 1 | **Multimodal understanding and vision generation results from our Janus**. Janus outperforms the previous state-of-the-art unified multimodal models as well as some task-specific multimodal understanding models, while also demonstrating strong visual generation capabilities. The image resolution is 384×384. Best viewed on screen.

derstanding and generation tasks, which improves instruction-following for visual generation, unlocks potential emergent abilities, and reduces model redundancy. Such methods typically use a single vision encoder to process inputs for both two tasks. However, the representations required by multimodal understanding and generation tasks differ significantly. In multimodal understanding tasks, the purpose of the vision encoder is to extract high-level semantic information (e.g., object categories or visual attributes within an image). The output of understanding task not only involves extracting information from images but also involves complex semantic reasoning. Therefore, the granularity of the vision encoder's representation tends to mainly focus on high-dimensional semantic representation. By contrast, in visual generation tasks, the main focus is on generating local details and maintaining global consistency in the image. The representation in this context necessitates a low-dimensional encoding that is capable of fine-grained spatial structure and textural detail expression. Unifying the representations of these two tasks within the same space will lead to conflicts and trade-offs. Consequently, existing unified models for multimodal understanding and generation often compromise on multimodal understanding performance, falling markedly short of the state-of-the-arts multimodal understanding models. We explore this issue further in the ablation study.

To solve this problem, we propose **Janus**[1], a unified multimodal framework that decouples visual encoding for multimodal understanding and generation. Specifically, we introduce two independent visual encoding pathways: one for multimodal understanding and one for multimodal generation, unified by the same transformer architecture. The proposed method offers two main benefits: (1) Janus alleviates the conflict stemming from the different granular needs of multimodal understanding and generation and eliminates the need to make trade-offs between two tasks when selecting visual encoders. (2) Janus is flexible and extensible. After decoupling, both the understanding and generation tasks can adopt state-of-the-art encoding

---

[1] In Roman mythology, Janus is the god of duality and transitions, symbolizing the coexistence of contradictory forces by having two faces, each looking in opposite directions. Similarly, our model captures the inherent tension between vision tasks: understanding demands abstract, high-level semantic representations, while generation requires concrete, detailed information. By decoupling these processes into specialized encoders, our system mirrors Janus's dual nature, resolving this tension within a unified architecture.

techniques specific to their domain. Moreover, it is possible for Janus to accommodate additional input types in the future, such as point clouds, EEG signals, or audio data, where independent encoders can extract features and then use a unified transformer to process them.

To the best of our knowledge, we are the first to highlight the importance of decoupling visual encoding within the unified multimodal understanding and generation framework. Our experimental results show that Janus surpasses existing unified models with comparable parameter sizes on both multimodal understanding and generation benchmarks, achieving state-of-the-art results. Notably, Janus even outperforms some task-specific models which have significantly more parameters (Figure 1). Specifically, on multimodal understanding benchmarks MMBench [54], SEED-Bench [42], and POPE [48], Janus (1.3B) achieved scores of 69.4, 63.7, and 87.0, respectively, outperforming LLaVA-v1.5 (7B) [50] and Qwen-VL-Chat (7B) [3] . On visual generation benchmarks MSCOCO-30K [11] and GenEval [30], Janus achieved an FID score of 8.53 and an accuracy of 61%, surpassing text-to-image generative models such as DALL-E 2 [66] and SDXL [62]. We believe that the strong performance, coupled with the high flexibility and extensibility of Janus, presents it as a strong candidate for next-generation unified multimodal models.

2. Related Work

2.1. Visual Generation

Visual generation is a rapidly evolving field that combines concepts from natural language processing with advancements in transformer architectures. Autoregressive models, influenced by the success in language processing, leverage transformers to predict sequences of discrete visual tokens (codebook IDs) [24, 65, 75]. These models tokenize visual data and employ a prediction approach similar to GPT-style [64] techniques. Additionally, masked prediction models [7, 8] draw upon BERT-style [19] masking methods, predicting masked sections of visual inputs to improve synthesis efficiency, and have been adapted for video generation [89]. Concurrently, continuous diffusion models have showcased impressive capabilities in visual generation [33, 67, 71], complementing discrete methods by approaching generation through a probabilistic lens.

2.2. Multimodal Understanding

Multimodal large language models (MLLMs) integrate both text and images [6, 80, 81]. By leveraging pretrained LLMs, MLLMs [1, 2, 12, 51, 55, 82, 95] demonstrate a robust ability to understand and process multimodal information. Recent advancements have explored extending MLLMs with pretrained diffusion models to facilitate image generation [27, 29, 36, 75, 76]. These methods fall under the category of tool utilization, where diffusion models are used to generate images based on the conditions output by the MLLM, while the MLLM itself does not have the ability to directly perform visual generation. Moreover, the generative ability of the entire system is often constrained by the external diffusion model, making its performance inferior to directly using the diffusion model on its own [27, 75].

2.3. Unified Multimodal Understanding and Generation

Unified multimodal understanding and generation models are considered powerful for facilitating seamless reasoning and generation across different modalities [77, 94]. Traditional approaches in these models typically use a single visual representation for both understanding

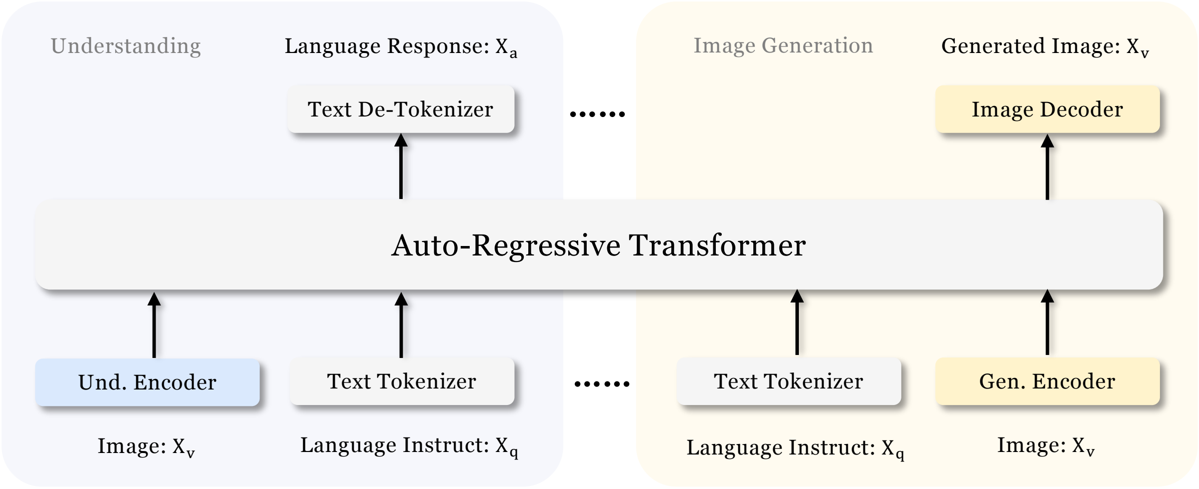

Figure 2 | **Architecture of our Janus.** Different from previous approaches [77, 85] that typically assume visual understanding and generation require the same visual encoder, our Janus decouples visual encoding for visual understanding and visual generation. "Und. Encoder" and "Gen. Encoder" are abbreviations for "Understanding Encoder" and "Generation Encoder", respectively. Best viewed in color.

and generation tasks, regardless of whether they are based on autoregressive (AR) models [77, 85] or diffusion models [86, 94]. For example, Chameleon [77] adopts a VQ Tokenizer to encode images for both multimodal understanding and generation. However, this practice may lead to suboptimal outcomes, as the vision encoder might face a trade-off between the demands of understanding and generation. In contrast, our Janus can explicitly decouple the visual representations for understanding and generation, recognizing that different tasks may require varying levels of information.

3. Janus: A Simple, Unified and Flexible Multimodal Framework

3.1. Architecture

The architecture of Janus is shown in Figure 2. For pure text understanding, multimodal understanding, and visual generation, we apply independent encoding methods to convert the raw inputs into features, which are then processed by an unified autoregressive transformer. Specifically, for text understanding, we use the built-in tokenizer of the LLM to convert the text into discrete IDs and obtain the feature representations corresponding to each ID. For multimodal understanding, we use the SigLIP [92] encoder to extract high-dimensional semantic features from images. These features are flattened from a 2-D grid into a 1-D sequence, and an understanding adaptor is used to map these image features into the input space of the LLM. For visual generation tasks, we use the VQ tokenizer from [73] to convert images into discrete IDs. After the ID sequence is flattened into 1-D, we use a generation adaptor to map the codebook embeddings corresponding to each ID into the input space of the LLM. We then concatenate these feature sequences to form a multimodal feature sequence, which is subsequently fed into the LLM for processing. The built-in prediction head of the LLM is utilized for text predictions in both the pure text understanding and multimodal understanding tasks, while a randomly initialized prediction head is used for image predictions in the visual generation task. The entire model adheres to an autoregressive framework without the need for specially designed

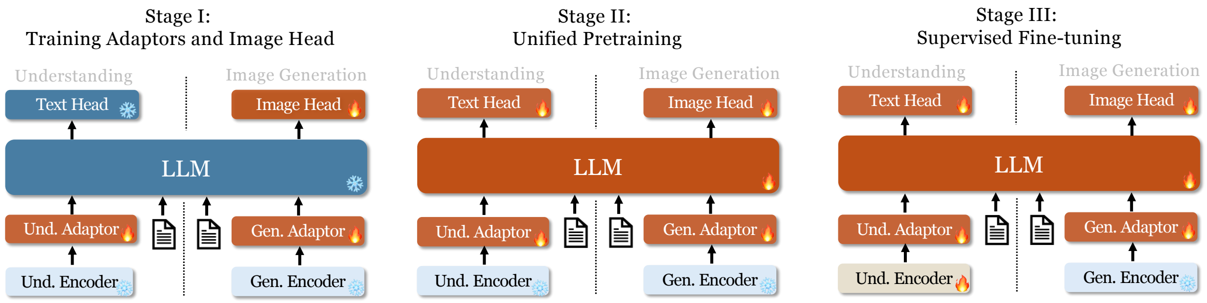

Figure 3 | **Our Janus adopts a three-stage training procedure.** We use flame symbols/snowflake symbols in the diagram to indicate the module updates/does not update its parameters.

attention masks.

3.2. Training Procedure

The training of Janus is divided into three stages, as illustrated in Figure 3. Details are provided in the below.

Stage I: Training Adaptors and Image Head. The main goal of this stage is to create a conceptual connection between visual and linguistic elements within the embedding space, enabling the LLM to understand the entities shown in images and have preliminary visual generation ability. We keep the visual encoders and the LLM frozen during this stage, allowing only the trainable parameters within the understanding adaptor, generation adaptor and image head to be updated.

Stage II: Unified Pretraining. In this stage, we perform unified pretraining with multimodal corpus to enable Janus to learn both multimodal understanding and generation. We unfreeze the LLM and utilize all types of training data: pure text data, multimodal understanding data, and visual generation data. Inspired by Pixart [9], we begin by conducting simple visual generation training using ImageNet-1k to help the model grasp basic pixel dependencies. Subsequently, we enhance the model's open-domain visual generation capability with general text-to-image data.

Stage III: Supervised Fine-tuning. During this stage, we fine-tune the pretrained model with instruction tuning data to enhance its instruction-following and dialogue capabilities. We fine-tune all parameters except the generation encoder. We focus on supervising the answers while masking system and user prompts. To ensure Janus's proficiency in both multimodal understanding and generation, we don't fine-tune separate models for a certain task. Instead, we use a blend of pure text dialogue data, multimodal understanding data and visual generation data, ensuring versatility across various scenarios.

3.3. Training Objective

Janus is an autoregressive model, and we simply adopt the cross-entropy loss during training:

$$\mathcal{L} = -\sum_{i=1} \log P_\theta(x_i | x_{<i}) \tag{1}$$

Here, $P(\cdot \mid \cdot)$ indicates the conditional probability modeled by the weights θ of Janus. For pure text understanding and multimodal understanding tasks, we compute the loss on the text sequence. For visual generation tasks, we compute the loss only on the image sequence. To keep the design simple, we have not assigned different loss weights to different tasks.

3.4. Inference

During inference, our model adopts a next-token prediction approach. For pure text understanding and multimodal understanding, we follow the standard practice of sampling tokens sequentially from the predicted distribution. For image generation, we utilize classifier-free guidance (CFG) [2], similar to prior works [8, 26, 73]. Specifically, for each token, the logit l_g is calculated as: $l_g = l_u + s(l_c - l_u)$, where l_c is the conditional logit, l_u is the unconditional logit, and s is the scale for the classifier-free guidance. The default number of s is 5 for the following evaluation.

3.5. Possible Extensions

It is important to note that our design, which features separate encoders for understanding and generation, is straightforward and easy to extend.

Multimodal Understanding. (1) For the multimodal understanding component, a stronger vision encoder can be chosen without worrying about whether the encoder is capable of handling vision generation tasks, such as EVA-CLIP [74], InternViT [13], etc. (2) To handle high-resolution images, dynamic high-resolution techniques [50] can be used. This allows the model to scale to any resolution, without performing positional embedding interpolation for ViTs. Tokens can be further compressed to save computational cost, for instance, using pixel shuffle operation [12].

Visual Generation. (1) For visual generation, finer-grained encoders can be chosen in order to preserve more image details after encoding, such as MoVQGan [93]. (2) Loss functions specifically designed for visual generation can be employed, such as diffusion loss [46]. (3) A combination of AR (causal attention) and parallel (bidirectional attention) methods can be used in the visual generation process to reduce accumulated errors during visual generation [79].

Support for Additional Modalities. The straightforward architecture of Janus allows for easy integration with additional encoders, accommodating various modalities such as 3D point cloud [53], tactile [88], and EEG [4]. This gives Janus the potential to become a more powerful multimodal generalist model.

4. Experiments

In this section, we present a series of comprehensive experiments designed to assess the performance of our method across a range of visual understanding and generation tasks. We begin by detailing our experimental setup, which includes the model architecture, training datasets, and evaluation benchmarks. Next, we report the performance of Janus, followed by a comparison with other state-of-the-art models on various benchmarks for multimodal understanding and generation. We also conduct extensive ablation studies to verify the effectiveness of the proposed method. Lastly, we provide some qualitative results.

---

[2] During training, we replace the text condition in the text-to-image data with a pad token at a probability of 10%, enabling the model to have unconditional visual generation capability.

Table 1 | **Detailed hyperparameters of our Janus**. Data ratio refers to the ratio of multimodal understanding data, pure text data, and visual generation data.

Hyperparameters	**Stage 1**	**Stage 2**	**Stage 3**
Learning rate	1.0×10^{-3}	1×10^{-4}	2.0×10^{-5}
LR scheduler	Cosine	Constant	Constant
Weight decay	0.0	0.0	0.1
Gradient clip	1.0	1.0	1.0
Optimizer	AdamW ($\beta_1 = 0.9, \beta_2 = 0.95$)		
Warm-up steps	300	5,000	0
Training steps	10,000	180,000	24,000
Batch size	256	512	256
Data Ratio	1 : 0 : 1	2 : 3 : 5	7 : 3 : 10

4.1. Implementation Details

In our experiments, we utilize DeepSeek-LLM (1.3B) [5] with a maximum supported sequence length of 4096 as the base language model. For the vision encoder used in understanding tasks, we select SigLIP-Large-Patch16-384 [92]. The generation encoder has a codebook of size 16,384 and downsamples images by a factor of 16. Both the understanding adaptor and the generation adaptor are two-layer MLPs. The detailed hyperparameters for each stage are provided in Table 1. All images are resized to 384×384 pixels. For multimodal understanding data, we resize the long side of the image and pad the short side with the background color (RGB: 127, 127, 127) to reach 384. For visual generation data, the short side is resized to 384, and the long side is cropped to 384. We use sequence packing during training to improve training efficiency. We mix all data types according to the specified ratios in a single training step. Our Janus is trained and evaluated using HAI-LLM [32], which is a lightweight and efficient distributed training framework built on top of PyTorch. The whole training process took 7 days on a cluster of 16 nodes, each equipped with 8 Nvidia A100 (40GB) GPUs.

4.2. Data Setup

In this section, we provide details of the pretraining and supervised finetuning datasets.

Stage I. We use a dataset that includes 1.25 million image-text paired captions from ShareGPT4V [10] for multimodal understanding and approximately 1.2 million samples from ImageNet-1k [18] for visual generation. The ShareGPT4V data is formatted as "`<image><text>`". The ImageNet data is organized into a text-to-image data format using the category names: "`<category_name><image>`". Here, the "<>" symbols represent placeholders.

Stage II. We organize the data into the following categories. (1) Text-only data. We use pre-training text copus from DeepSeek-LLM [5]. (2) Interleaved image-text data. We use Wiki-How [39] and WIT [72] dataset. (3) Image caption data. We use images from [17, 18, 23, 38, 40, 45, 47, 49, 70]. Among them, we employ open-source multimodal model to re-caption images in [17, 40]. The image caption data is formatted into question-answer pairs, for example, "`<image>Describe the image in detail.<caption>`". (4) Table and chart data. We use corresponding table and chart data from DeepSeek-VL [55]. The data is formatted as "`<question><answer>`". (5) Visual generation data. We utilize image-caption pairs from various datasets including [17, 38, 40, 57, 58, 60, 63, 70], along with 2M in-house data. For images from [38, 70], we filter based on aesthetic scores and image sizes, resulting in 20% remaining. During training, we randomly use only the first sentence of a caption with a 25% probability to

Table 2 | **Comparison with state-of-the-arts on multimodal understanding benchmarks**. "Und." and "Gen." denote "understanding" and "generation", respectively. Models using external pretrained diffusion model are marked with †.

Type	Model	# LLM Params	POPE↑	MME-P↑	MMB↑	SEED↑	VQAv2$_{(test)}$↑	GQA↑	MMMU↑	MM-Vet↑
Und. Only	LLaVA-v1.5-Phi-1.5 [86]	1.3B	84.1	1128.0	-	-	75.3	56.5	30.7	-
	MobileVLM [14]	1.4B	84.5	1196.2	53.2	-	-	56.1	-	-
	MobileVLM-V2 [15]	1.4B	84.3	1302.8	57.7	-	-	59.3	-	-
	MobileVLM [14]	2.7B	84.9	1288.9	59.6	-	-	59.0	-	-
	MobileVLM-V2 [15]	2.7B	84.7	1440.5	63.2	-	-	61.1	-	-
	LLaVA-Phi [96]	2.7B	85.0	1335.1	59.8	-	71.4	-	-	28.9
	LLaVA [51]	7B	76.3	809.6	38.7	33.5	-	-	-	25.5
	LLaVA-v1.5 [50]	7B	85.9	1510.7	64.3	58.6	78.5	62.0	35.4	31.1
	InstructBLIP [16]	7B	-	-	36.0	53.4	-	49.2	-	26.2
	Qwen-VL-Chat [3]	7B	-	1487.5	60.6	58.2	78.2	57.5	-	-
	IDEFICS-9B [41]	8B	-	-	48.2	-	50.9	38.4	-	-
	Emu3-Chat [83]	8B	85.2	-	58.5	68.2	75.1	60.3	31.6	-
	InstructBLIP [16]	13B	78.9	1212.8	-	-	-	49.5	-	25.6
Und. and Gen.	DreamLLM† [21]	7B	-	-	-	-	72.9	-	-	36.6
	LaVIT† [36]	7B	-	-	-	-	66.0	46.8	-	-
	Emu† [75]	13B	-	-	-	-	52.0	-	-	-
	NExT-GPT† [84]	13B	-	-	-	-	66.7	-	-	-
	Show-o [86]	1.3B	73.8	948.4	-	-	59.3	48.7	25.1	-
	Gemini-Nano-1 [78]	1.8B	-	-	-	-	62.7	-	26.3	-
	LWM [52]	7B	75.2	-	-	-	55.8	44.8	-	9.6
	VILA-U [85]	7B	85.8	1401.8	-	59.0	79.4	60.8	-	33.5
	Chameleon [77]	7B	-	-	-	-	-	-	22.4	8.3
	Janus (Ours)	1.3B	87.0	1338.0	69.4	63.7	77.3	59.1	30.5	34.3

encourage the model to develop strong generation capabilities for short descriptions. ImageNet samples [18] are presented only during the first 120K training steps, while images from other datasets appear in the later 60K steps. This approach helps the model first learn basic pixel dependencies before progressing to more complex scene understanding, as suggested by [9]. The visual generation data is provided in the format: "`<caption><image>`".

Stage III. For text understanding, we use data from [43]. For multimodal understanding, we use instruct tuning data from [31, 34, 35, 43, 56, 69]. For visual generation, we use image-text pairs from [17, 60, 70] (a subset of that in stage II) and 4M in-house data. We utilize the following format for instruction tuning:"`User:<Input Message> \n Assistant: <Response>`". For multi-turn dialogues, we repeat this format to structure the data.

4.3. Evaluation Setup

Multimodal Understanding. To assess multimodal understanding capabilities, we evaluate our model on widely recognized image-based vision-language benchmarks, which include VQAv2 [31], GQA [35], POPE [48], MME [25], SEED [42], MMB [54], MM-Vet [90], and MMMU [91].

Visual Generation. For evaluating visual generation capabilities, we use the MSCOCO-30K [11], MJHQ-30K [44], and GenEval [30] benchmarks. MSCOCO-30K and MJHQ-30K employ the Fréchet Inception Distance (FID) metric on generated images compared to 30K high-quality images, which indicates the overall efficacy of image generation. GenEval is a challenging benchmark for image-to-text generation, designed to reflect the comprehensive generative

Table 3 | **Evaluation of text-to-image generation ability on GenEval benchmark**. "Und." and "Gen." denote "understanding" and "generation", respectively. Models using external pretrained diffusion model are marked with †.

Type	Method	# Params	Single Obj.	Two Obj.	Counting	Colors	Position	Color Attri.	Overall↑
Gen. Only	LlamaGen [73]	0.8B	0.71	0.34	0.21	0.58	0.07	0.04	0.32
	LDM [67]	1.4B	0.92	0.29	0.23	0.70	0.02	0.05	0.37
	SDv1.5 [67]	0.9B	0.97	0.38	0.35	0.76	0.04	0.06	0.43
	PixArt-α [9]	0.6B	0.98	0.50	0.44	0.80	0.08	0.07	0.48
	SDv2.1 [67]	0.9B	0.98	0.51	0.44	0.85	0.07	0.17	0.50
	DALL-E 2 [66]	6.5B	0.94	0.66	0.49	0.77	0.10	0.19	0.52
	Emu3-Gen [83]	8B	0.98	0.71	0.34	0.81	0.17	0.21	0.54
	SDXL [62]	2.6B	0.98	0.74	0.39	0.85	0.15	0.23	0.55
Und. and Gen.	SEED-X† [29]	17B	0.97	0.58	0.26	0.80	0.19	0.14	0.49
	Show-o [86]	1.3B	0.95	0.52	0.49	0.82	0.11	0.28	0.53
	LWM [52]	7B	0.93	0.41	0.46	0.79	0.09	0.15	0.47
	Chameleon [77]	34B	-	-	-	-	-	-	0.39
	Janus (Ours)	1.3B	0.97	0.68	0.30	0.84	0.46	0.42	0.61

abilities of visual generation models by offering a detailed instance-level analysis of their compositional capabilities.

4.4. Comparison with State-of-the-arts

Multimodal Understanding Performance. We compare the proposed method with state-of-the-art unified models and understanding-only models in Table 2. Janus achieves the overall best results among models of similar scale. Specifically, compared to the previous best unified model, Show-o [86], we achieve performance improvements of 41% (949 → 1338) and 30% (48.7 → 59.1) on the MME and GQA datasets, respectively. This can be attributed to Janus decoupling the visual encoding for multimodal understanding and generation, mitigating the conflict between these two tasks. When compared to models with significantly larger sizes, Janus remains highly competitive. For instance, Janus outperforms LLaVA-v1.5 (7B) on several datasets, including POPE, MMbench, SEED Bench, and MM-Vet.

Visual Generation Performance. We report visual generation performance on GenEval, COCO-30K and MJHQ-30K benchmarks. As shown in Table 3, our Janus obtains 61% overall accuracy on GenEval, which outperforms the previous best unified model Show-o (53%) and some popular generation-only methods, e.g., SDXL (55%) and DALL-E 2 (52%). This demonstrates that our approach has better instruction-following capabilities. As shown in Table 4, Janus achieves FIDs of 8.53 and 10.10 on the COCO-30K and MJHQ-30K benchmarks, respectively, surpassing unified models Show-o and LWM, and demonstrating competitive performance compared to some well-known generation-only methods. This demonstrates that the images generated by Janus have good quality and highlights its potential in visual generation.

4.5. Ablation Studies

We carefully design ablation studies to verify the effectiveness of Janus's design concept. First, we design experiments to validate the importance and benefits of decoupling visual encoding. Second, we investigate the impact of unified training on individual tasks like multimodal understanding or visual generation. Results are listed in Table 5.

Table 4 | **Evaluation of text-to-image generation ability on MSCOCO-30K and MJHQ-30K benchmark**. "Und." and "Gen." denote "understanding" and "generation", respectively. Models using external pretrained diffusion model are marked with †.

Type	Model	# Params	COCO-30K↓	MJHQ-30K↓
Gen. Only	DALL·E [65]	12B	27.50	-
	GLIDE [59]	5B	12.24	-
	LDM [67]	1.4B	12.64	-
	DALL·E 2 [66]	6.5B	10.39	-
	SDv1.5 [67]	0.9B	9.62	-
	GigaGAN [37]	0.9B	9.09	-
	PixArt-α [9]	0.6B	7.32	-
	Imagen [68]	34B	7.27	-
	RAPHAEL [87]	3B	6.61	-
Und. and Gen.	Emu† [75]	13B	11.66	-
	NExT-GPT† [84]	13B	11.28	-
	SEED-X† [29]	17B	14.99	-
	Show-o [86]	1.3B	9.24	15.18
	LWM [52]	7B	12.68	17.77
	VILA-U (256) [85]	7B	-	12.81
	VILA-U (384) [85]	7B	-	7.69
	Janus (Ours)	1.3B	8.53	10.10

Table 5 | **Ablation studies**. We verify the effectiveness of decoupling visual encoding and compare unified training with task-specific training. "Und.", "Gen." and "SE. Tokenizer" denote "understanding", "generation" and "semantic tokenizer", respectively.

Exp ID	Visual Encoder	Training Task	POPE↑	MMB↑	SEED↑	MMMU↑	COCO-FID↓
A	VQ Tokenizer	Und. + Gen.	60.1	35.0	34.9	24.7	8.72
B	SE. Tokenizer	Und. + Gen.	82.4	52.7	54.9	26.6	7.11
C	SE. Tokenizer	Und.	83.9	62.1	60.8	27.5	-
D	SigLIP + VQ (Ours)	Und. + Gen.	87.0	69.4	63.7	30.5	8.53
E	SigLIP	Und.	85.9	70.6	64.8	28.8	-
F	VQ Tokenizer	Gen.	-	-	-	-	8.92

Baseline Construction. Following previous work [77], we select a VQ tokenizer [73] to encode images for both multimodal understanding and generation tasks, serving as the baseline (Exp-A). Considering that the VQ tokenizer in Exp-A might be weak in extract semantic information, making it less effective for multimodal understanding, we also construct a stronger baseline Exp-B. We adopt SigLIP to distill an enhanced semantic tokenizer [3] that can extract high-level semantic information from images while also have the ability to convert images into discrete IDs, which is similar to that in [85]. Details of the semantic tokenizer could be found in the Appendix A.1.

Impact of Decoupling Visual Encoding. (1) From the results of Exp-A, we find the model achieves satisfactory performance on visual generation benchmark (8.72 FID on COCO). However, there is a significant gap on understanding benchmarks between Exp-A and our model (Exp-D). (2) When comparing Exp-B to Exp-A, the results show a clear improvement in multi-

---

[3] The semantic tokenizer is only used in the ablation study as a stronger baseline. For simplicity, we use the ordinary VQ tokenizer [73] in the main experiment.

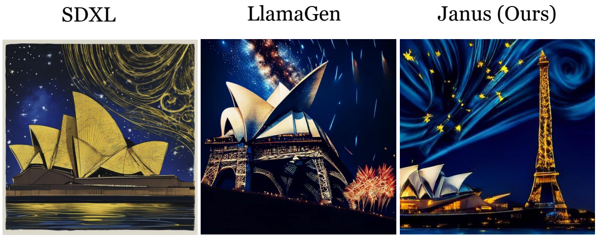

A close-up high-contrast photo of Sydney Opera House sitting next to Eiffel tower, under a blue night sky of roiling energy, exploding yellow stars, and radiating swirls of blue.

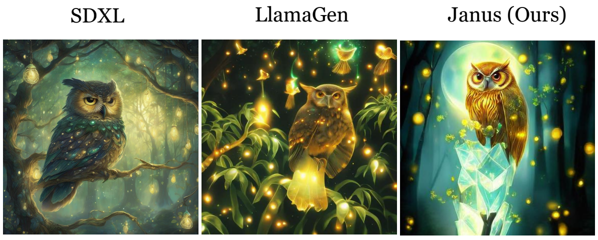

A wise old owl with golden plumage perched on a luminous crystal tree in a magical forest. Radiant fireflies swirl around while ethereal mist rolls through the trees, illuminated by swirls of iridescent moonlight and glistening emerald leaves.

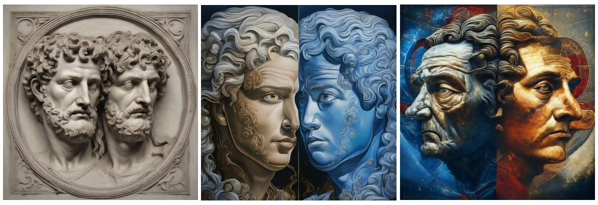

A detailed portrait of the Roman god Janus, featuring his two faces looking in opposite directions. One face appears aged, with deep-set wrinkles and a wise, contemplative expression, while the other face is youthful, exuding vigor and curiosity. His hair is styled in flowing curls, framing both faces with a sense of divine symmetry. The artwork is rich in contrasting colors, with the left side dominated by cold blues and silvers, symbolizing winter and reflection, and the right side awash with warm golds and reds, representing spring and renewal. The background is a celestial tapestry, adorned with stars and symbolic motifs of time and passage.

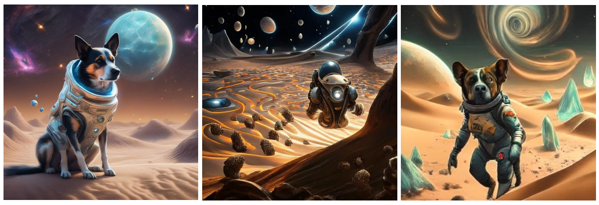

A brave dog wearing a futuristic space suit, exploring an alien planet amidst swirling dunes of stardust and meteor showers. The landscape is dotted with glowing crystal formations and ethereal terraforms, creating a surreal environment in which swirling vortexes in the sky depict the endless dance of distant galaxies.

Figure 4 | **Qualitative comparisons of visual generation with LlamaGen and SDXL**. The images generated by Janus show better consistency with the user's prompts. The image resolutions for SDXL, LlamaGen, and ours are 1024×1024, 512×512, and 384×384, respectively. Best viewed on screen.

modal understanding, although there is still a considerable gap compared to our method. In terms of visual generation, Exp-B outperforms Exp-D. We hypothesize two possible reasons for this. First, the semantic tokenizer produces discrete IDs that are more semantically coherent, providing more reasonable prediction targets for the LLM. Second, the visual encoder in Exp-B has significantly more parameters than the Gen. encoder in Exp-D. (3) To investigate whether using a single visual encoder leads to a trade-off between multimodal understanding and generation, we further design Exp-C based on Exp-B, which focuses solely on multimodal understanding training. The multimodal understanding ability of Exp-C is significantly better than that of Exp-B. This indicates that the visual encoder in Exp-B made trade-offs between multimodal understanding and generation, ultimately sacrificing its multimodal understanding capability. The above experiments illustrate the importance of decoupling visual encoding.

Unified Model vs. Pure Understanding & Pure Generation. We compare the performance of unified training (Exp-D) against pure understanding (Exp-E) and pure generation (Exp-F) training. For pure understanding, we omit visual generation data. For pure generation, we exclude the understanding data. Please note that unified training and pure understanding training go through the same steps for the understanding part. Similarly, unified training and pure generation training go through the same steps for the visual generation part. Experimental results show that the performance of unified training is comparable to that of training solely for understanding or solely for visual generation. This demonstrates that our model, Janus, is capable of incorporating strong generative abilities while minimally affecting multimodal understanding performance.

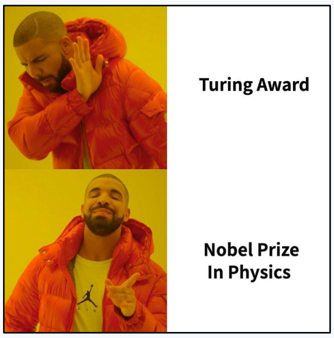

User: What is the meaning of this meme from the top panel to the bottom?

Janus (Ours): The meme is a humorous take on the concept of a Nobel Prize in Physics. The top panel shows a man in a red jacket with his hand up, seemingly confused or surprised, while the bottom panel shows the same man with a smile on his face, seemingly pleased or proud, as if he has just won the Nobel Prize. The meme is a play on the idea that the man in the top panel might be confused or surprised by the idea of winning a Nobel Prize in Physics, while the man in the bottom panel seems to be genuinely happy about it.

Chameleon: The meme is a visual representation of a conversation between two people, with the top panel featuring the text "I'm not arguing, I'm just explaining why I'm right" and the bottom panel featuring the text "No, you're not." The meme is using a technique called "irony" to convey the idea that even though one person is presenting themselves as non-argumentative, they are actually being argumentative. The use of the phrase "I'm not arguing, I'm just explaining why I'm right" is a common tactic used by people who are trying to avoid an argument but are actually engaging in one. The meme is poking fun at this tactic by showing the person's actions and words as being in direct contradiction to their claim.

Show-o: The meaning of the meme from the top panel to the bottom is that it is a humorous and light-hearted depiction of a man wearing a yellow hat and a red jacket, with the caption "I'm not a fan of the sun." This suggests that the man is not a fan of the sun, and he is using the sun as a metaphor for his feelings or emotions. The meme is likely meant to be humorous and entertaining, as it combines a serious subject with a lighthearted and playful approach

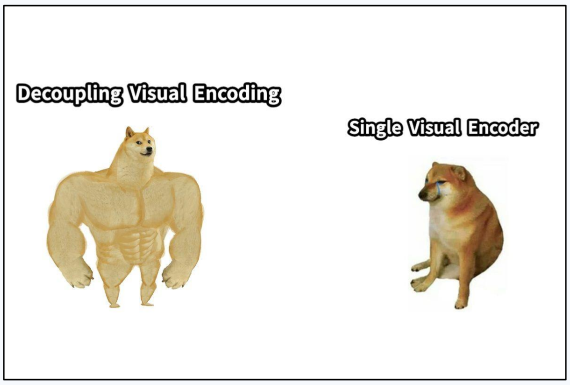

User: Explain this meme.

Janus (Ours): The meme is comparing two different types of neural networks used in machine learning. The first type is called "Decoupling Visual Encoding," and the second type is called "Single Visual Encoder." The meme is trying to convey that the first type is more powerful and can handle more complex tasks, while the second type is simpler and less powerful.

Chameleon: This image shows a cartoon of a pig and a bear side-by-side, with the text "When you're a vegan and your friends still order sausage and bacon" above them. The image is a humorous take on the challenges of being a vegan in a non-vegan environment, where one's friends or family may not share their dietary preferences.

Show-o: The image features two dogs, one brown and one white, standing side by side. The brown dog is positioned on the left side of the image, while the white dog is on the right. Both dogs are looking at the camera, seemingly posing for a picture. The brown dog is slightly larger than the white dog. The image is captioned with the phrase "I'm not a dog, but I'm a dog." This humorous statement is accompanied by the image of the two dogs, emphasizing their ...

Figure 5 | **Qualitative results of multimodal understanding on humorous memes**. We compare the response with Chameleon-7B [77] and Show-o [86]. We emphasize the key-points in the response. Best viewed on screen.

4.6. Qualitative Results

Visualizations of Visual Generation. Figure 4 provides qualitative comparisons between our model, diffusion-based models like SDXL [62], and the autoregressive model LlamaGen [73].

The results show that our model demonstrates superior instruction-following capabilities in visual generation, accurately capturing most of details in the user's prompt. This indicates the potential of the unified model in the realm of visual generation. More visualizations can be found in the Appendix B.

Multimodal Understanding on MEME Images. Figure 5 showcases the qualitative results of Janus's multimodal understanding ability, compared with Chameleon [77] and Show-o [86]. Janus accurately interprets the text caption and captures the emotion conveyed in the meme. In contrast, both Chameleon and Show-o struggle with accurately recognizing the text in the image. Additionally, Chameleon fails to identify objects in the meme, while Show-o misinterprets the dog's color. These examples highlight that the decoupled vision encoder significantly enhances Janus's fine-grained multimodal understanding ability compared to the shared encoder used by Chameleon and Show-o. More multimodal understanding exmples can be found in the Appendix B.

5. Conclusion

In this paper, we introduced Janus, a simple, unified and extensible multimodal understanding and generation model. The core idea of Janus is to decouple visual encoding for multimodal understanding and generation, which could alleviate the conflict arising from the differing demands that understanding and generation place on the visual encoder. Extensive experiments have demonstrated the effectiveness and leading performance of Janus. It is also worth noting that Janus is flexible and easy to extend. In addition to having significant potential for improvement in both multimodal understanding and generation, Janus is also easily extendable to incorporate more input modalities. The above advantages suggest that Janus may serve as an inspiration for the development of the next generation of multimodal general-purpose models.

Appendix

A. Details of Semantic Tokenizer Mentioned in Ablation Study

A.1. Architecture of Semantic Tokenizer

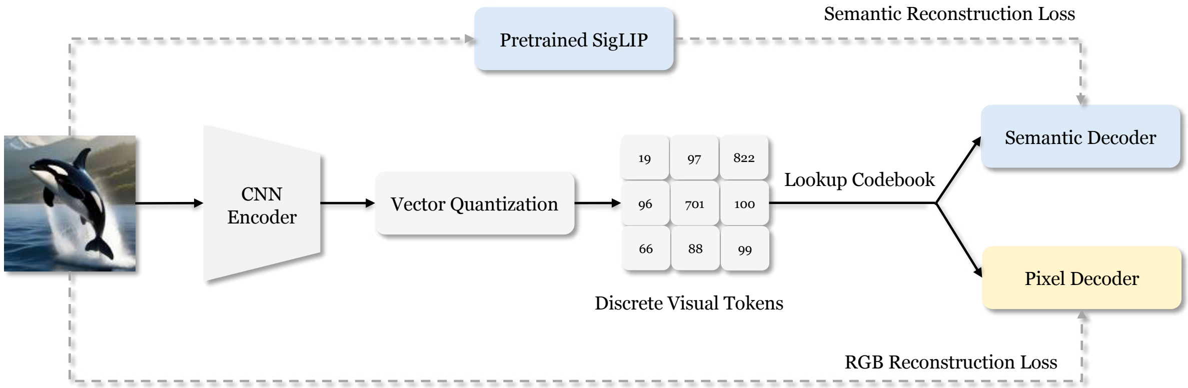

(a) Architecture of Semantic Tokenizer

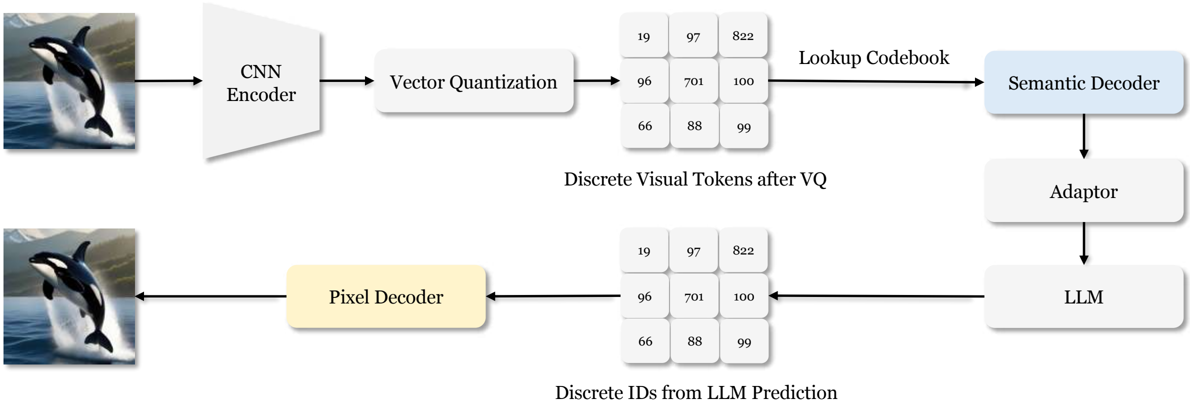

(b) Architecture of LLM with Semantic Tokenizer Integration

Figure 6 | **Architecture and usage of the semantic tokenizer.** (a) Architecture used during training of the semantic tokenizer. We use pre-trained SigLIP [92] to supervise the reconstruction of semantic information, while using raw image to supervise the reconstruction of RGB values. (b) Integrating LLM with the semantic decoder. The semantic decoder outputs continuous features with high-level semantics, which are passed through an adaptor and then used as input for the LLM. Please note that the semantic tokenizer is only used in the ablation study, not in the main experiment.

We build the semantic tokenizer based on the tokenizer architecture proposed in [73], which has a downsample rate of 16. In addition to the original CNN pixel decoder, we add an additional semantic decoder branch after Vector Quantization, as shown in Figure 6 (a). The semantic decoder is a 12-layer ViT [22], with 12 attention heads and a hidden dimension of 768. For the semantic decoder, we use a causal attention mask to facilitate next token prediction when integrating it with an LLM.

A.2. Training

Training Procedure. The semantic tokenizer is trained from scratch in a two-stage manner. In the first stage, we train the model on the ImageNet-1k [18] dataset for 40 epochs. In the second stage, we fine-tune the model for 1 epoch on 50 million images. These images come from the visual generation data used during the Janus pretraining process. We use a constant learning rate of $1e-4$ and a batch size of 128.

Training Loss. The training loss of the semantic tokenizer consists of two parts. On one hand, we use the loss for RGB reconstruction as described in [73]. On the other hand, we use SigLIP-Large-Patch16-384 as the teacher to supervise the semantic feature reconstruction results by the semantic decoder. We adopt the loss in BEiT-v2 [61]. Specifically, we maximize the cosine similarity between the semantic feature predicted by the semantic decoder and the SigLIP output. The weight for the semantic reconstruction loss is set to 0.25.

A.3. Integrating with LLM

We present the integration of the semantic tokenizer and the LLM in Figure 6 (b). The image is first transformed into continuous features through the CNN encoder, vector quantization and the semantic decoder. Then, the LLM processes these features and generates predictions for the image IDs. Finally, the pixel decoder converts these discrete IDs into RGB values.

B. Additional Qualitative Results

More Visualizations of Text-to-Image Generation. We present more text-to-image generation results in Figure 7. It is evident that Janus is capable of producing high-quality images that adhere closely to the given prompts. We further explore the multilingual text-to-image capabilities of our model, as shown in Figure 8. We are pleasantly surprised to find that, despite our training data consisting solely of English text-to-image data, Janus can still process text-to-image tasks in other languages. We attribute this multilingual ability to the original large language model's inherent traits. The LLM initially translates various languages into a unified semantic space, allowing Janus to perform text-to-image tasks naturally without additional training.

More Multimodal Understanding Results. Additional results on multimodal understanding are shown in Figure 9. Janus exhibits impressive comprehension abilities when handling inputs from various contexts, showcasing its powerful capabilities.

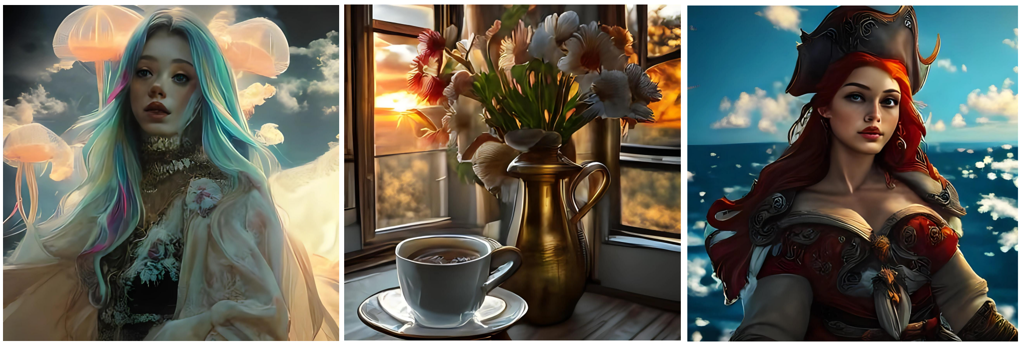

a young woman, looks like mix of Lana Del Rey and grimes, flowing cool colored hair, marbled, iridescent, shoujo manga, pre-raphaelite, k-pop, gilded, pearl, spun silk, clouds, ghost, glowing jellyfish, billowing gossamer cloth, Alexander McQueen, handmade lace, floral embroidery, snakeskin, dramatic lighting

Real photo of a cup of hot steaming coffee and a brass vase with a large bouquet of spring flowers by an old oak window at sunrise, fine details, rich colors taken with a nikon z6 camera and a nikon nikkor lens with 50 f5.6 iso 100 and a shutter speed of 1400 knot. UHD dtm HDR 8k

Portrait of a beautiful, curvaceous, Pirate princess goddess babe, red hair, intricate ornate costume, Caribbean background + outdoors + Ocean, painted by ArtGerm, Alphonse Mucha, Roberto Ferri, Ross Tran, Pixar, low angle shot, digital painting, cinematic rim lighting, Unreal Engine 5, 8K

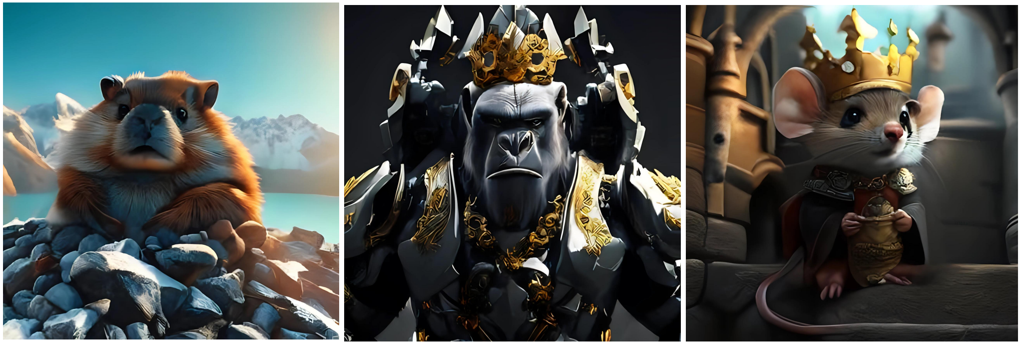

a cute fluffy chubby marmot sunbathing on a pile of rocks, snow mountains background, turquoise glacier lake afar, clear blue sky, highly detailed, golden hour, natural light, octane render, unreal engine

epic 3d portrait of white King Kong wearing mech armor made of black crystals, golden ornate around the armor, symmetrical body, hyperrealistic, intricate details, shiny, cinematic, unreal engine, artstation, octane render,

Tiny cute adorable mouse dressed as a king in a castle, anthropomorphic, Jean-Baptiste Monge, soft cinematic lighting, 8k, intricate details, portrait, Pixar style character, old fashioned movie style

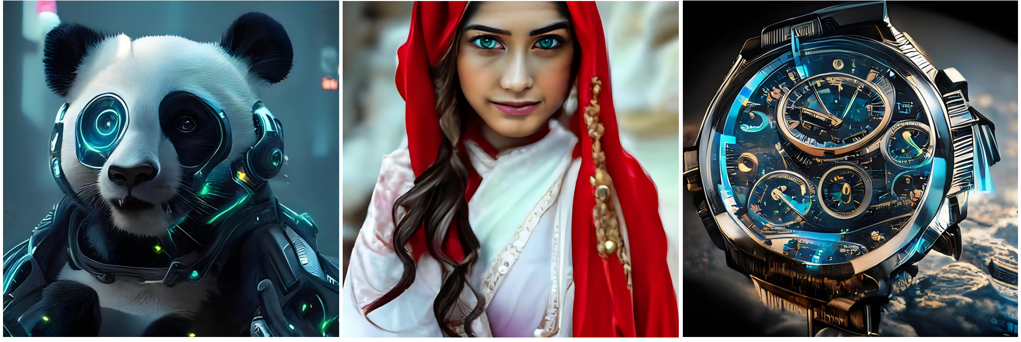

a panda that has been cybernetically enhanced more cybernetics3d 4k unreal engine chaos 20

A stunning princess from kabul in red, white traditional clothing, blue eyes, brown hair.

The ultimate wrist watch watch time machine , super advanced technology, holographic display, intricate mechanism.

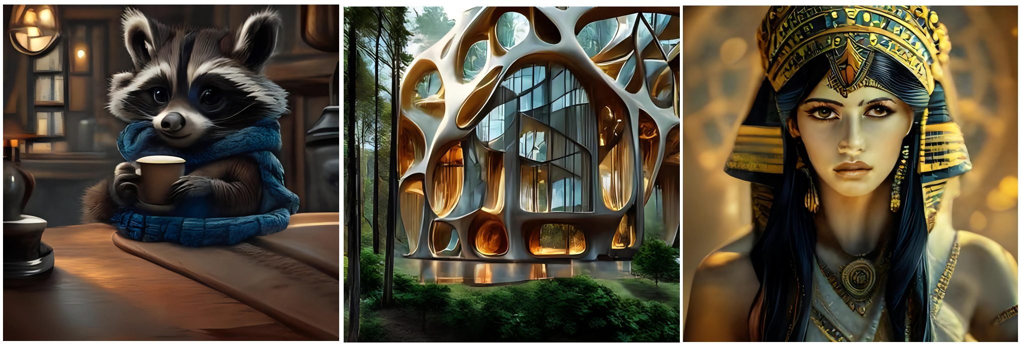

Tiny cute adorable fluffy baby raccoon with knitted blue scarf leaning at a table in a medieval pub holding a coffee cup, anthropomorphic, Jean-Baptiste Monge, soft cinematic lighting, 8k, intricate details, portrait, Pixar style character, old fashioned movie style

Architectural parametric pavilion made from wood and glass, with organic cavities, surrounded by a beautiful forest. Dramatic scene, photorealistic, hyperrealistic, raytracing reflections, 8k hd, intrincate detail in the style of Frank Lloyde Wright

Beautiful surreal symbolism the mesmerizing vision of a Cleopatra Queen of Egypt , full body , mesmerizing brown eyes, black hair and ethereal features, radiating celestial aura, super high definition, true lifelike color, perfect exposure, razor sharp focus, golden ratio, soft reflections, bokeh effect, fine art photography, cinematic compositing, authentic, professional by Rorianai style 36k s1000

Figure 7 | More text-to-image generation results. We upsample the images to 1024 × 1024 for better visualization.

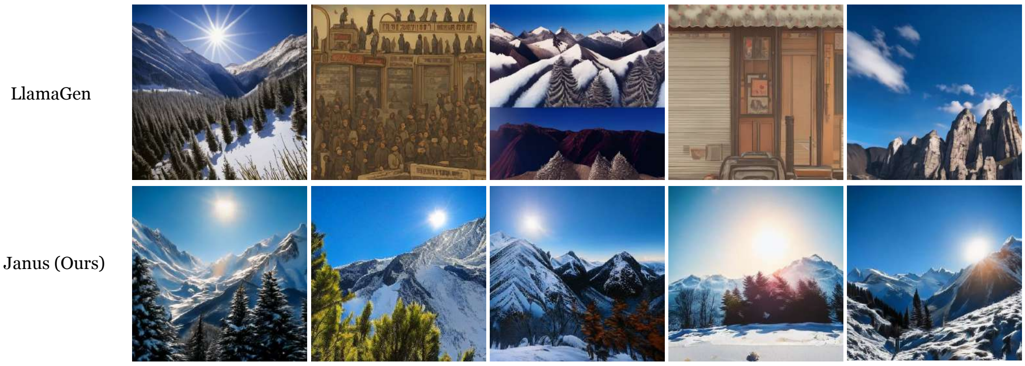

A realistic photo of snowy mountains with sunlit peaks glistening under a clear blue sky

这是一张雪山写实照片，阳光照耀下的山峰在晴朗的蓝天下熠熠生辉。前景中高大的常青树被白雪覆盖，为这令人惊叹的高山景色增添了深度。

Une photo réaliste de montagnes enneigées dont les sommets éclairés par le soleil scintillent sous un ciel bleu limpide. Au premier plan, de grands arbres à feuilles persistantes saupoudrés de neige ajoutent de la profondeur à cette scène alpine à couper le souffle.

澄み切った青空の下、太陽に照らされた山頂が輝く雪山のリアルな写真。前景の雪に覆われた背の高い常緑樹が、息をのむようなアルプスの風景に深みを与えている。

A realistic photo of ❄️ 🏔️ with ☀️ under a clear blue sky. Tall, snow-dusted 🌲 in the foreground add depth to the breathtaking alpine scene.

Figure 8 | Multilingual text-to-image generation samples compared to LlamaGen [73]. Note that we only use English text-to-image data in training, and this is an emergent capability of our model. The languages used in the prompt, from left to right, are: English, Chinese, French, Japanese, and English with emoji.

Prompt

Generate the latex code of this formula.

$$A_n = a_0 \left[1 + \frac{3}{4} \sum_{k=1}^{n} \left(\frac{4}{9} \right)^k \right]$$

Response

A _ { n } = a_ 0 \left[1 + \frac{3}{4} \sum_{ k=1}^{n} \left(\frac{4}{9} \right)^k \right]

Prompt

Generate the matplotlib.pyplot code for this plot.

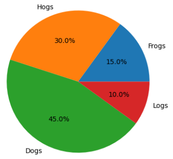

Response

The image you've provided is a pie chart that represents the distribution of different types of animals based on their frequency. The chart is divided into four segments, each representing a different type of animal and its corresponding percentage.
Here's the code to generate the pie chart:

~~~
```python
import matplotlib.pyplot as plt
# Data
animals = [
   {"name": "Hogs", "frequency": 30.0},
   {"name": "Frog", "frequency": 15.0},
   {"name": "Logs", "frequency": 10.0},
   {"name": "Dogs", "frequency": 45.0}
]
# Create the pie chart
plt.pie(animals, labels=animals, autopct='%1.1f%%',
startangle=90)
# Set the title and labels
plt.title('Distribution of Animals')
plt.title.set_text('Frequency of Animals')
# Show the plot
plt.show()
```
~~~

Prompt

What algorithm does the image depict?

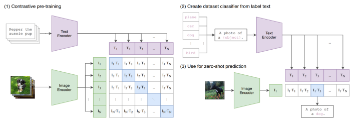
(1) Contrastive pre-training
Pepper the aussie pup
Text Encoder
Image Encoder
T_1 T_2 T_3 ... T_N
I_1 I_2 I_3 ⋮ I_N
$I_1 \cdot T_1$ $I_1 \cdot T_2$ $I_1 \cdot T_3$ ... $I_1 \cdot T_N$
$I_2 \cdot T_1$ $I_2 \cdot T_2$ $I_2 \cdot T_3$ ... $I_2 \cdot T_N$
$I_3 \cdot T_1$ $I_3 \cdot T_2$ $I_3 \cdot T_3$ ... $I_3 \cdot T_N$
$I_N \cdot T_1$ $I_N \cdot T_2$ $I_N \cdot T_3$ ... $I_N \cdot T_N$
(2) Create dataset classifier from label text
plane
car
dog
bird
A photo of a {object}.
Text Encoder
(3) Use for zero-shot prediction
Image Encoder
I_1
A photo of a dog.

Figure 1. Summary of our approach. While standard image models jointly train an image feature extractor and a linear classifier to predict some label, CLIP jointly trains an image encoder and a text encoder to predict the correct pairings of a batch of (image, text) training examples. At test time the learned text encoder synthesizes a zero-shot linear classifier by embedding the names or descriptions of the target dataset's classes.

Response

The image depicts a CLIP (Contrastive Language-Image Pre-training) model. The CLIP model is a type of pre-training algorithm that combines the power of language and vision to learn a unified representation of the world. The image encoder processes the input image, and the text encoder processes the text associated with the image. The output of the text encoder is then used to predict the correct pair of images, which is a key component of the CLIP model.

Prompt

Why is this painting interesting?

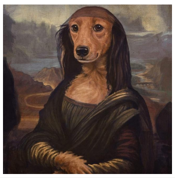

Response

This image is an interesting piece of art because it combines a well-known painting, the "Mona Lisa," with a dog. The dog is depicted in the same pose as the Mona Lisa, but with a different expression and a different background. The painting is a unique blend of art styles and subjects, making it stand out.

Figure 9 | More multimodal understanding results. Janus has a strong multimodal understanding capability and can handle inputs from various contexts, such as scientific charts, artwork images, LaTeX formula images, and more.

References

[1] J. Achiam, S. Adler, S. Agarwal, L. Ahmad, I. Akkaya, F. L. Aleman, D. Almeida, J. Altenschmidt, S. Altman, S. Anadkat, et al. Gpt-4 technical report. arXiv preprint arXiv:2303.08774, 2023.

[2] Anthropic. The claude 3 model family: Opus, sonnet, haiku. `https://www.anthropic.com`, 2024.

[3] J. Bai, S. Bai, S. Yang, S. Wang, S. Tan, P. Wang, J. Lin, C. Zhou, and J. Zhou. Qwen-vl: A frontier large vision-language model with versatile abilities. arXiv preprint arXiv:2308.12966, 2023.

[4] Y. Bai, X. Wang, Y.-p. Cao, Y. Ge, C. Yuan, and Y. Shan. Dreamdiffusion: Generating high-quality images from brain eeg signals. arXiv preprint arXiv:2306.16934, 2023.

[5] X. Bi, D. Chen, G. Chen, S. Chen, D. Dai, C. Deng, H. Ding, K. Dong, Q. Du, Z. Fu, et al. Deepseek llm: Scaling open-source language models with longtermism. arXiv preprint arXiv:2401.02954, 2024.

[6] T. B. Brown. Language models are few-shot learners. arXiv preprint arXiv:2005.14165, 2020.

[7] H. Chang, H. Zhang, L. Jiang, C. Liu, and W. T. Freeman. Maskgit: Masked generative image transformer. In Proceedings of the IEEE/CVF Conference on Computer Vision and Pattern Recognition, pages 11315–11325, 2022.

[8] H. Chang, H. Zhang, J. Barber, A. Maschinot, J. Lezama, L. Jiang, M.-H. Yang, K. Murphy, W. T. Freeman, M. Rubinstein, et al. Muse: Text-to-image generation via masked generative transformers. arXiv preprint arXiv:2301.00704, 2023.

[9] J. Chen, J. Yu, C. Ge, L. Yao, E. Xie, Y. Wu, Z. Wang, J. Kwok, P. Luo, H. Lu, et al. Pixart-$alpha$: Fast training of diffusion transformer for photorealistic text-to-image synthesis. arXiv preprint arXiv:2310.00426, 2023.

[10] L. Chen, J. Li, X. Dong, P. Zhang, C. He, J. Wang, F. Zhao, and D. Lin. Sharegpt4v: Improving large multi-modal models with better captions. arXiv preprint arXiv:2311.12793, 2023.

[11] X. Chen, H. Fang, T.-Y. Lin, R. Vedantam, S. Gupta, P. Dollár, and C. L. Zitnick. Microsoft coco captions: Data collection and evaluation server. arXiv preprint arXiv:1504.00325, 2015.

[12] Z. Chen, W. Wang, H. Tian, S. Ye, Z. Gao, E. Cui, W. Tong, K. Hu, J. Luo, Z. Ma, et al. How far are we to gpt-4v? closing the gap to commercial multimodal models with open-source suites. arXiv preprint arXiv:2404.16821, 2024.

[13] Z. Chen, J. Wu, W. Wang, W. Su, G. Chen, S. Xing, M. Zhong, Q. Zhang, X. Zhu, L. Lu, et al. Internvl: Scaling up vision foundation models and aligning for generic visual-linguistic tasks. In Proceedings of the IEEE/CVF Conference on Computer Vision and Pattern Recognition, pages 24185–24198, 2024.

[14] X. Chu, L. Qiao, X. Lin, S. Xu, Y. Yang, Y. Hu, F. Wei, X. Zhang, B. Zhang, X. Wei, et al. Mobilevlm: A fast, reproducible and strong vision language assistant for mobile devices. arXiv preprint arXiv:2312.16886, 2023.

[15] X. Chu, L. Qiao, X. Zhang, S. Xu, F. Wei, Y. Yang, X. Sun, Y. Hu, X. Lin, B. Zhang, et al. Mobilevlm v2: Faster and stronger baseline for vision language model. arXiv preprint arXiv:2402.03766, 2024.

[16] W. Dai, J. Li, D. Li, A. M. H. Tiong, J. Zhao, W. Wang, B. Li, P. Fung, and S. Hoi. Instructblip: Towards general-purpose vision-language models with instruction tuning, 2023.

[17] dclure. Laion-aesthetics-umap. `https://huggingface.co/datasets/dclure/laion-aesthetics-12m-umap`, 2022.

[18] J. Deng, W. Dong, R. Socher, L.-J. Li, K. Li, and L. Fei-Fei. Imagenet: A large-scale hierarchical image database. In 2009 IEEE conference on computer vision and pattern recognition, pages 248–255. Ieee, 2009.

[19] J. Devlin. Bert: Pre-training of deep bidirectional transformers for language understanding. arXiv preprint arXiv:1810.04805, 2018.

[20] P. Dhariwal and A. Nichol. Diffusion models beat gans on image synthesis. Advances in neural information processing systems, 34:8780–8794, 2021.

[21] R. Dong, C. Han, Y. Peng, Z. Qi, Z. Ge, J. Yang, L. Zhao, J. Sun, H. Zhou, H. Wei, et al. Dreamllm: Synergistic multimodal comprehension and creation. arXiv preprint arXiv:2309.11499, 2023.

[22] A. Dosovitskiy. An image is worth 16x16 words: Transformers for image recognition at scale. arXiv preprint arXiv:2010.11929, 2020.

[23] Echo840. Detailed caption dataset. `https://huggingface.co/datasets/echo840/Detailed_Caption`, 2023.

[24] P. Esser, R. Rombach, and B. Ommer. Taming transformers for high-resolution image synthesis. In Proceedings of the IEEE/CVF conference on computer vision and pattern recognition, pages 12873–12883, 2021.

[25] C. Fu, P. Chen, Y. Shen, Y. Qin, M. Zhang, X. Lin, J. Yang, X. Zheng, K. Li, X. Sun, et al. Mme: A comprehensive evaluation benchmark for multimodal large language models. arXiv preprint arXiv:2306.13394, 2023.

[26] O. Gafni, A. Polyak, O. Ashual, S. Sheynin, D. Parikh, and Y. Taigman. Make-a-scene: Scene-based text-to-image generation with human priors. In European Conference on Computer Vision, pages 89–106. Springer, 2022.

[27] Y. Ge, Y. Ge, Z. Zeng, X. Wang, and Y. Shan. Planting a seed of vision in large language model. arXiv preprint arXiv:2307.08041, 2023.

[28] Y. Ge, S. Zhao, Z. Zeng, Y. Ge, C. Li, X. Wang, and Y. Shan. Making llama see and draw with seed tokenizer. arXiv preprint arXiv:2310.01218, 2023.

[29] Y. Ge, S. Zhao, J. Zhu, Y. Ge, K. Yi, L. Song, C. Li, X. Ding, and Y. Shan. Seed-x: Multimodal models with unified multi-granularity comprehension and generation. arXiv preprint arXiv:2404.14396, 2024.

[30] D. Ghosh, H. Hajishirzi, and L. Schmidt. Geneval: An object-focused framework for evaluating text-to-image alignment. Advances in Neural Information Processing Systems, 36, 2024.

[31] Y. Goyal, T. Khot, D. Summers-Stay, D. Batra, and D. Parikh. Making the v in vqa matter: Elevating the role of image understanding in visual question answering. In Proceedings of the IEEE conference on computer vision and pattern recognition, pages 6904–6913, 2017.

[32] High-flyer. Hai-llm: Efficient and lightweight training tool for large models, 2023. URL https://www.high-flyer.cn/en/blog/hai-llm.

[33] J. Ho, A. Jain, and P. Abbeel. Denoising diffusion probabilistic models. Advances in neural information processing systems, 33:6840–6851, 2020.

[34] Y.-C. Hsiao, F. Zubach, M. Wang, et al. Screenqa: Large-scale question-answer pairs over mobile app screenshots. arXiv preprint arXiv:2209.08199, 2022.

[35] D. A. Hudson and C. D. Manning. Gqa: A new dataset for real-world visual reasoning and compositional question answering. In Proceedings of the IEEE/CVF conference on computer vision and pattern recognition, pages 6700–6709, 2019.

[36] Y. Jin, K. Xu, L. Chen, C. Liao, J. Tan, B. Chen, C. Lei, A. Liu, C. Song, X. Lei, et al. Unified language-vision pretraining with dynamic discrete visual tokenization. arXiv preprint arXiv:2309.04669, 2023.

[37] M. Kang, J.-Y. Zhu, R. Zhang, J. Park, E. Shechtman, S. Paris, and T. Park. Scaling up gans for text-to-image synthesis. In Proceedings of the IEEE/CVF Conference on Computer Vision and Pattern Recognition, pages 10124–10134, 2023.

[38] A. Kirillov, E. Mintun, N. Ravi, H. Mao, C. Rolland, L. Gustafson, T. Xiao, S. Whitehead, A. C. Berg, W.-Y. Lo, et al. Segment anything. In Proceedings of the IEEE/CVF International Conference on Computer Vision, pages 4015–4026, 2023.

[39] M. Koupaee and W. Y. Wang. Wikihow: A large scale text summarization dataset. arXiv preprint arXiv:1810.09305, 2018.

[40] A. Kuznetsova, H. Rom, N. Alldrin, J. Uijlings, I. Krasin, J. Pont-Tuset, S. Kamali, S. Popov, M. Malloci, A. Kolesnikov, T. Duerig, and V. Ferrari. The open images dataset v4: Unified image classification, object detection, and visual relationship detection at scale. IJCV, 2020.

[41] H. Laurençon, D. van Strien, S. Bekman, L. Tronchon, L. Saulnier, T. Wang, S. Karamcheti, A. Singh, G. Pistilli, Y. Jernite, and et al. Introducing idefics: An open reproduction of state-of-the-art visual language model, 2023. URL https://huggingface.co/blog/idefics.

[42] B. Li, R. Wang, G. Wang, Y. Ge, Y. Ge, and Y. Shan. Seed-bench: Benchmarking multimodal llms with generative comprehension. arXiv preprint arXiv:2307.16125, 2023.

[43] B. Li, Y. Zhang, D. Guo, R. Zhang, F. Li, H. Zhang, K. Zhang, Y. Li, Z. Liu, and C. Li. Llava-onevision: Easy visual task transfer. arXiv preprint arXiv:2408.03326, 2024.

[44] D. Li, A. Kamko, E. Akhgari, A. Sabet, L. Xu, and S. Doshi. Playground v2. 5: Three insights towards enhancing aesthetic quality in text-to-image generation. arXiv preprint arXiv:2402.17245, 2024.

[45] L. Li, Y. Wang, R. Xu, P. Wang, X. Feng, L. Kong, and Q. Liu. Multimodal arxiv: A dataset for improving scientific comprehension of large vision-language models. arXiv preprint arXiv:2403.00231, 2024.

[46] T. Li, Y. Tian, H. Li, M. Deng, and K. He. Autoregressive image generation without vector quantization. arXiv preprint arXiv:2406.11838, 2024.

[47] X. Li, F. Zhang, H. Diao, Y. Wang, X. Wang, and L.-Y. Duan. Densefusion-1m: Merging vision experts for comprehensive multimodal perception. arXiv preprint arXiv:2407.08303, 2024.

[48] Y. Li, Y. Du, K. Zhou, J. Wang, W. X. Zhao, and J.-R. Wen. Evaluating object hallucination in large vision-language models. arXiv preprint arXiv:2305.10355, 2023.

[49] Z. Li, X. Yang, K. Choi, W. Zhu, R. Hsieh, H. Kim, J. H. Lim, S. Ji, B. Lee, X. Yan, et al. Mmsci: A multimodal multi-discipline dataset for phd-level scientific comprehension. arXiv preprint arXiv:2407.04903, 2024.

[50] H. Liu, C. Li, Y. Li, and Y. J. Lee. Improved baselines with visual instruction tuning. In Proceedings of the IEEE/CVF Conference on Computer Vision and Pattern Recognition, pages 26296–26306, 2024.

[51] H. Liu, C. Li, Q. Wu, and Y. J. Lee. Visual instruction tuning. Advances in neural information processing systems, 36, 2024.

[52] H. Liu, W. Yan, M. Zaharia, and P. Abbeel. World model on million-length video and language with ringattention. arXiv preprint arXiv:2402.08268, 2024.

[53] M. Liu, R. Shi, K. Kuang, Y. Zhu, X. Li, S. Han, H. Cai, F. Porikli, and H. Su. Openshape: Scaling up 3d shape representation towards open-world understanding. Advances in neural information processing systems, 36, 2024.

[54] Y. Liu, H. Duan, Y. Zhang, B. Li, S. Zhang, W. Zhao, Y. Yuan, J. Wang, C. He, Z. Liu, et al. Mmbench: Is your multi-modal model an all-around player? arXiv preprint arXiv:2307.06281, 2023.

[55] H. Lu, W. Liu, B. Zhang, B. Wang, K. Dong, B. Liu, J. Sun, T. Ren, Z. Li, Y. Sun, et al. Deepseek-vl: towards real-world vision-language understanding. arXiv preprint arXiv:2403.05525, 2024.

[56] P. Lu, L. Qiu, J. Chen, T. Xia, Y. Zhao, W. Zhang, Z. Yu, X. Liang, and S.-C. Zhu. Iconqa: A new benchmark for abstract diagram understanding and visual language reasoning. arXiv preprint arXiv:2110.13214, 2021.

[57] madebyollin. Megalith-huggingface. https://huggingface.co/datasets/madebyollin/megalith-10m, 2024.

[58] mehdidc. Yfcc-huggingface. https://huggingface.co/datasets/mehdidc/yfcc15m, 2024.

[59] A. Nichol, P. Dhariwal, A. Ramesh, P. Shyam, P. Mishkin, B. McGrew, I. Sutskever, and M. Chen. Glide: Towards photorealistic image generation and editing with text-guided diffusion models. arXiv preprint arXiv:2112.10741, 2021.

[60] J. Pan, K. Sun, Y. Ge, H. Li, H. Duan, X. Wu, R. Zhang, A. Zhou, Z. Qin, Y. Wang, J. Dai, Y. Qiao, and H. Li. Journeydb: A benchmark for generative image understanding, 2023.

[61] Z. Peng, L. Dong, H. Bao, Q. Ye, and F. Wei. Beit v2: Masked image modeling with vector-quantized visual tokenizers. arXiv preprint arXiv:2208.06366, 2022.

[62] D. Podell, Z. English, K. Lacey, A. Blattmann, T. Dockhorn, J. Müller, J. Penna, and R. Rombach. Sdxl: Improving latent diffusion models for high-resolution image synthesis. arXiv preprint arXiv:2307.01952, 2023.

[63] ProGamerGov. Dalle3-high-quality-captions. `https://huggingface.co/datasets/ProGamerGov/synthetic-dataset-1m-dalle3-high-quality-captions`, 2024.

[64] A. Radford. Improving language understanding by generative pre-training. 2018.

[65] A. Ramesh, M. Pavlov, G. Goh, S. Gray, C. Voss, A. Radford, M. Chen, and I. Sutskever. Zero-shot text-to-image generation. In International conference on machine learning, pages 8821–8831. Pmlr, 2021.

[66] A. Ramesh, P. Dhariwal, A. Nichol, C. Chu, and M. Chen. Hierarchical text-conditional image generation with clip latents. arXiv preprint arXiv:2204.06125, 1(2):3, 2022.

[67] R. Rombach, A. Blattmann, D. Lorenz, P. Esser, and B. Ommer. High-resolution image synthesis with latent diffusion models. In Proceedings of the IEEE/CVF conference on computer vision and pattern recognition, pages 10684–10695, 2022.

[68] C. Saharia, W. Chan, S. Saxena, L. Li, J. Whang, E. L. Denton, K. Ghasemipour, R. Gontijo Lopes, B. Karagol Ayan, T. Salimans, et al. Photorealistic text-to-image diffusion models with deep language understanding. Advances in neural information processing systems, 35:36479–36494, 2022.

[69] S. Shah, A. Mishra, N. Yadati, and P. P. Talukdar. Kvqa: Knowledge-aware visual question answering. In Proceedings of the AAAI conference on artificial intelligence, volume 33, pages 8876–8884, 2019.

[70] V. Singla, K. Yue, S. Paul, R. Shirkavand, M. Jayawardhana, A. Ganjdanesh, H. Huang, A. Bhatele, G. Somepalli, and T. Goldstein. From pixels to prose: A large dataset of dense image captions. arXiv preprint arXiv:2406.10328, 2024.

[71] J. Song, C. Meng, and S. Ermon. Denoising diffusion implicit models. arXiv preprint arXiv:2010.02502, 2020.

[72] K. Srinivasan, K. Raman, J. Chen, M. Bendersky, and M. Najork. Wit: Wikipedia-based image text dataset for multimodal multilingual machine learning. In Proceedings of the 44th international ACM SIGIR conference on research and development in information retrieval, pages 2443–2449, 2021.

[73] P. Sun, Y. Jiang, S. Chen, S. Zhang, B. Peng, P. Luo, and Z. Yuan. Autoregressive model beats diffusion: Llama for scalable image generation. arXiv preprint arXiv:2406.06525, 2024.

[74] Q. Sun, Y. Fang, L. Wu, X. Wang, and Y. Cao. Eva-clip: Improved training techniques for clip at scale. arXiv preprint arXiv:2303.15389, 2023.

[75] Q. Sun, Q. Yu, Y. Cui, F. Zhang, X. Zhang, Y. Wang, H. Gao, J. Liu, T. Huang, and X. Wang. Generative pretraining in multimodality. arXiv preprint arXiv:2307.05222, 2023.

[76] Q. Sun, Y. Cui, X. Zhang, F. Zhang, Q. Yu, Y. Wang, Y. Rao, J. Liu, T. Huang, and X. Wang. Generative multimodal models are in-context learners. In Proceedings of the IEEE/CVF Conference on Computer Vision and Pattern Recognition, pages 14398–14409, 2024.

[77] C. Team. Chameleon: Mixed-modal early-fusion foundation models. arXiv preprint arXiv:2405.09818, 2024.

[78] G. Team, R. Anil, S. Borgeaud, Y. Wu, J.-B. Alayrac, J. Yu, R. Soricut, J. Schalkwyk, A. M. Dai, A. Hauth, et al. Gemini: a family of highly capable multimodal models. arXiv preprint arXiv:2312.11805, 2023.

[79] K. Tian, Y. Jiang, Z. Yuan, B. Peng, and L. Wang. Visual autoregressive modeling: Scalable image generation via next-scale prediction. arXiv preprint arXiv:2404.02905, 2024.

[80] H. Touvron, T. Lavril, G. Izacard, X. Martinet, M.-A. Lachaux, T. Lacroix, B. Rozière, N. Goyal, E. Hambro, F. Azhar, et al. Llama: Open and efficient foundation language models. arXiv preprint arXiv:2302.13971, 2023.

[81] H. Touvron, L. Martin, K. Stone, P. Albert, A. Almahairi, Y. Babaei, N. Bashlykov, S. Batra, P. Bhargava, S. Bhosale, et al. Llama 2: Open foundation and fine-tuned chat models. arXiv preprint arXiv:2307.09288, 2023.

[82] W. Wang, Z. Chen, X. Chen, J. Wu, X. Zhu, G. Zeng, P. Luo, T. Lu, J. Zhou, Y. Qiao, et al. Visionllm: Large language model is also an open-ended decoder for vision-centric tasks. Advances in Neural Information Processing Systems, 36, 2024.

[83] X. Wang, X. Zhang, Z. Luo, Q. Sun, Y. Cui, J. Wang, F. Zhang, Y. Wang, Z. Li, Q. Yu, et al. Emu3: Next-token prediction is all you need. arXiv preprint arXiv:2409.18869, 2024.

[84] S. Wu, H. Fei, L. Qu, W. Ji, and T.-S. Chua. Next-gpt: Any-to-any multimodal llm. arXiv preprint arXiv:2309.05519, 2023.

[85] Y. Wu, Z. Zhang, J. Chen, H. Tang, D. Li, Y. Fang, L. Zhu, E. Xie, H. Yin, L. Yi, et al. Vila-u: a unified foundation model integrating visual understanding and generation. arXiv preprint arXiv:2409.04429, 2024.

[86] J. Xie, W. Mao, Z. Bai, D. J. Zhang, W. Wang, K. Q. Lin, Y. Gu, Z. Chen, Z. Yang, and M. Z. Shou. Show-o: One single transformer to unify multimodal understanding and generation. arXiv preprint arXiv:2408.12528, 2024.

[87] Z. Xue, G. Song, Q. Guo, B. Liu, Z. Zong, Y. Liu, and P. Luo. Raphael: Text-to-image generation via large mixture of diffusion paths. Advances in Neural Information Processing Systems, 36, 2024.

[88] F. Yang, C. Ma, J. Zhang, J. Zhu, W. Yuan, and A. Owens. Touch and go: Learning from human-collected vision and touch. arXiv preprint arXiv:2211.12498, 2022.

[89] L. Yu, Y. Cheng, K. Sohn, J. Lezama, H. Zhang, H. Chang, A. G. Hauptmann, M.-H. Yang, Y. Hao, I. Essa, et al. Magvit: Masked generative video transformer. In Proceedings of the IEEE/CVF Conference on Computer Vision and Pattern Recognition, pages 10459–10469, 2023.

[90] W. Yu, Z. Yang, L. Li, J. Wang, K. Lin, Z. Liu, X. Wang, and L. Wang. Mm-vet: Evaluating large multimodal models for integrated capabilities. arXiv preprint arXiv:2308.02490, 2023.

[91] X. Yue, Y. Ni, K. Zhang, T. Zheng, R. Liu, G. Zhang, S. Stevens, D. Jiang, W. Ren, Y. Sun, et al. Mmmu: A massive multi-discipline multimodal understanding and reasoning benchmark for expert agi. In Proceedings of the IEEE/CVF Conference on Computer Vision and Pattern Recognition, pages 9556–9567, 2024.

[92] X. Zhai, B. Mustafa, A. Kolesnikov, and L. Beyer. Sigmoid loss for language image pre-training. In Proceedings of the IEEE/CVF International Conference on Computer Vision, pages 11975–11986, 2023.

[93] C. Zheng, T.-L. Vuong, J. Cai, and D. Phung. Movq: Modulating quantized vectors for high-fidelity image generation. Advances in Neural Information Processing Systems, 35: 23412–23425, 2022.

[94] C. Zhou, L. Yu, A. Babu, K. Tirumala, M. Yasunaga, L. Shamis, J. Kahn, X. Ma, L. Zettlemoyer, and O. Levy. Transfusion: Predict the next token and diffuse images with one multi-modal model. arXiv preprint arXiv:2408.11039, 2024.

[95] D. Zhu, J. Chen, X. Shen, X. Li, and M. Elhoseiny. Minigpt-4: Enhancing vision-language understanding with advanced large language models. arXiv preprint arXiv:2304.10592, 2023.

[96] Y. Zhu, M. Zhu, N. Liu, Z. Ou, X. Mou, and J. Tang. Llava-phi: Efficient multi-modal assistant with small language model. arXiv preprint arXiv:2401.02330, 2024.